FERMILAB-PUB-17-525-PPD
ACCEPTED

Structure and luminescence properties of Dy_2O_3 doped bismuth-borate glasses

C. Mugoni[a*], C. Gatto[b], A. Pla-Dalmau[c], C. Siligardi[a]

[a]Department of Engineering "Enzo Ferrari", University of Modena and Reggio Emilia, Via P. Vivarelli 10/1, 41125, Modena, Italy

[b]Istituto Nazionale Di Fisica Nucleare, Sezione di Napoli, Italy

[c]Fermi National Accelerator Laboratory, Batavia, IL 60510 United States

*corresponding author; e-mail address: consuelo.mugoni@unimore.it; tel: +39 0592056282; fax: +39 0592056243.

Abstract

In this work heavy bismuth-borate glasses were studied as host matrices of Dy_2O_3 rare earth, for potential application as scintillator materials in high energy physics experiments and in general radiation detection systems. Glass matrices were prepared from 20BaO - xBi_2O_3 – $(80\text{-}x)B_2O_3$ (x= 20, 30, 40 mol%) ternary systems and synthesized by the melt-quenching method at different temperatures in order to obtain high density and high transparency in the UV/Vis range. Particularly, the glass manifesting the higher transparency and with sufficiently high density was doped with Dy_2O_3 (2.5 and 5 mol%) in order to induce the luminescence characteristics. The effects of Bi_2O_3 and Dy_2O_3 on density, thermal behaviour, transmission as well as luminescence properties under UV excitation, were investigated. The experimental results show that the synthesized glasses can be considered promising candidate materials as dense scintillators, due to the Dy^{3+} centres emission.

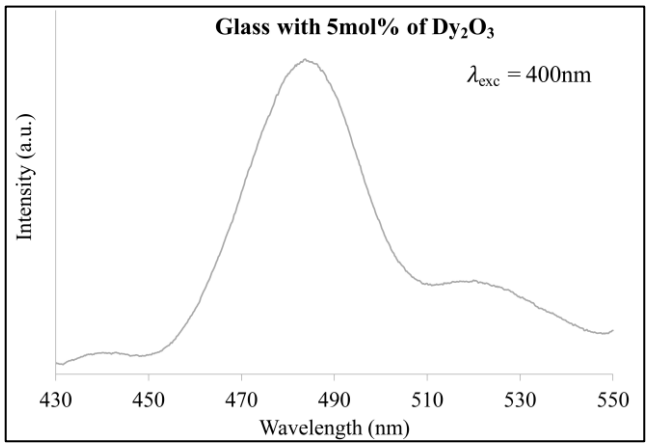

Keywords: luminescence, heavy glasses, density, calorimeter, high energy physics

1. Introduction

Inorganic glasses are potential sources of affordable scintillators for particle physics. However, in calorimetric applications for high energy physics other specific properties such as high density and high transparency, over the near-ultraviolet and visible regions, need to be possessed [1,2]. In fact, larger densities results in an increased radiation absorption cross-section and, consequently, an improved signal-to-noise ratio [3-6], while high transparency avoids losses through light scattering caused by heterogeneities like grain boundaries, composition gradients and lattice imperfections. Glasses containing rare earths are promising alternatives to single crystals and ceramic and plastic scintillators due to their low-cost production and ease of manufacturing in different sizes and shapes [5]. The main disadvantage of existing oxide glass scintillators is their low density, typically below 4 g/cm^3 [7,8], that significantly limits their applications in radiation detectors. However, the introduction of heavy components such as lead as PbO or PbF_2 and Bi_2O_3 allows the density of the glasses to be easily increased to more than 6.0 g/cm^3, that is desirable for the most applications. In spite of the above mentioned advantages, lead containing glasses are considered to be toxic and incompatible with the principles of green chemistry and sustainable development [9]. Consequently, they are currently being removed from various practical applications and replaced by others glass systems such as bismuthate glasses [10] and germanate glasses [11].

The aim of this work is the development of a glassy material with high density and luminescent properties. Particularly, barium bismuth borate glasses containing dysprosium as rare earth were synthesized via the melt-quenching method. Boron oxide was selected as glass former for its extensive glass formation range, high transparency, high thermal and radiation

stability [12]. The melting process was conducted in a Pt crucible instead of alumina to avoid any possible reaction with the borate melts that could potentially lead to drastic decrease of the final density by destruction of tetrahedral boron species [13,14]. The transparent glasses were characterized in terms of density, molar volume, X-Ray Diffraction (XRD), differential thermal analysis (DTA), UV-VIS spectroscopy and luminescence properties.

2. Method

Homogeneous glasses belonging to $20BaO\text{-}xBi_2O_3\text{-}(80\text{-}x)B_2O_3$ system (BB series) and doped with different amounts of Dy_2O_3 ($20BaO\text{-}(x\text{-}y)Bi_2O_3\text{-}yDy_2O_3\text{-}(80\text{-}x\text{-}y)B_2O_3$, BBD series) were prepared by the following procedure. Firstly, appropriate amount of $BaCO_3$ (Alfa Aesar, 99.99%), Bi_2O_3 (Alfa Aesar, 99.99%), H_3BO_3 (Alfa Aesar, 99.99%) and Dy_2O_3 (Alfa Aesar, 99.99%) were mixed for 15 minutes in an alumina jar, according to the target glass composition (**Tables 1** and **2**), and synthesized by the melt-quenching method. Melting of the glasses was performed in an electrical furnace (Lenton, mod. EHF 17/17) under air atmosphere. Subsequently, the melt was poured onto a graphite mould and the obtained bulk samples were annealed at 10°C below their glass transition temperature (T_g) in order to relieve the thermal stress and to reduce the number of the defects thus, improving the transmittance of the final glassy materials.

In detail, the glasses belonging to BB series were synthesized at different melting temperatures 950, 1050, 1100 and 1200°C for 1 hour as illustrated in **Table 1**, with a heating cycle of 10°C per minutes from room to the melting temperatures. Different melting temperatures were tested in order to monitor the aesthetic properties of glasses in terms of colour and transparency, considering their well-known dependence on the oxidation-reduction equilibrium of bismuth. Subsequently, the glass with the higher transparency and a sufficiently high density (BB20) was selected as the host matrix for scintillating Dy_2O_3.

Different amounts of Dy_2O_3 (2.5 and 5 mol %) were added to the batch compositions, replacing Bi_2O_3 (**Table 2**) and the raw materials were melted at 1050°C employing three different holding times (1, 3 and 6 h). In this way, the effect of melting duration on glasses transparency and homogeneity was monitored, according with recent scientific literature [15]. The densities of the glass specimens were measured by the Archimedes method on five different samples for each glass composition. The molar volume (V_M) and the oxygen packing density (O) of each glass were evaluated from the density (ρ) and the molecular weight (M) according to the following eq. (1) and eq. (2) respectively:

$$V_M = (\Sigma_i n_i M_i) / \rho \quad (1)$$

$$O = (\rho/M) \times n, \quad (2)$$

where n_i is the molar fraction of the oxide component, i, M_i its molecular weight, and d is the glass density and n is the number of oxygen atoms per formula unit.

The mineralogical analysis was performed by X-ray diffraction (XRD) in order to understand the nature of the studied samples. XRD patterns were collected using a powder diffractometer (Philips PW3710) with a Ni-filtered Cu Kα radiation in the 10-80° 2θ range, step size 0.02° and 3s time step. The thermal properties of the glassy materials were determined with a Netzsch, STA 409 differential thermal analyser (DTA) on sample ground to an average particle size of less than 30 μm. The DTA measurements were carried out on *ca.* 30 mg of sample in a Pt crucible. Bulk samples of 1x1x1 cm^3 were prepared and polished with SiC abrasive papers and 0.03 μm alumina paste in order to decrease the surface roughness, that is desired for the optical and luminescence properties. UV–visible absorption spectra were acquired in the wavelength range of 200 – 1100 nm by using Ocean Optics HR4000CG-UV-NIR spectrophotometer equipped with ocean optics DH-2000-BAL (Balanced Deuterium Tungsten Halogen Light Source) lamp. The absorption coefficient, α (ω) was calculated as a function of wavelength considering the following equation:

$$\ln T = -\alpha t \quad (3)$$

where t is the sample thickness.

The band gap was determined from the UV-Vis spectra by considering the relationship reported below:

$$(\alpha h\upsilon)^n = h\upsilon - E_{opt} \quad (4)$$

where α is an energy independent constant, E_{opt} is optical band gap energy and the exponent n=1/2 denote the allowed direct transition.

The theoretical optical basicity (Λ_{th}) was, also, calculated on the basis of the following equation proposed by Duffy and Ingram [16]

$$\Lambda_{th} = X_1\Lambda_1 + X_2\Lambda_2 + \ldots X_n\Lambda_n \quad (5)$$

where X_1, X_2,..., and X_n are equivalent fractions based on the amount of oxygen in each oxide contributing to the overall material stoichiometry and Λ_1, Λ_2,..., and Λ_n are the basicities assigned to the individual oxides.

The luminescence properties under UV excitation were studied with a UV-Vis spectrophotometer. The emitted scintillating light has been detected by a photodetector (either a PMT or an SiPM) and recorded with a custom Data Acquisition (DAQ) systems (PADE) developed by Fermilab Electronics support group. The resolution of fluorescence excitation and emission measurements is 0.2 nm.

3. Results

The obtained glasses were transparent and completely free of bubbles, except those melted at 1200°C. In the BB series the colour changed with the composition and the melting temperature (**Table 1**). In particular, it varied from pale yellow to amber by increasing the amount of Bi_2O_3 or the temperature from 950 to 1100°C, becoming dark at 1200°C independently by the starting composition. The synthesis of BB series conducted at 1050°C allowed obtaining at the same time transparent, homogeneous and high density samples thus,

in the present paper the following discussion is focused on these glasses. Among these, the BB-20 glass (containing 20 mol% of Bi_2O_3) was selected as the best glass matrix to accommodate Dy_2O_3 (BBD series) for their higher transparency and homogeneity with respect to the other glasses as well as high density. The substitution of Bi_2O_3 by 2.5 and 5 mol% of Dy_2O_3 in the BBD series does not produce any significant change in the glass colour.

3.1 X-Ray powder diffraction (XRD)

The X-Ray powder diffraction confirmed the vitreous nature of all the samples obtained at 1050°C. In **Figure 1** the spectrum of BB-20 is illustrated as an example. The bands detected at approximately 25-30 °2theta and 45-50 °2theta, are typical of a borate glass structure where BO_3 and BO_4 units coexist [17].

3.2 Density (ρ)**, molar volume (V_M) and packing oxygen (O)**

Density of glass is generally explained in terms of competition between the masses and the volumes of the various structural groups present in it. Therefore, density is related to how tightly the atoms and atomic groups are placed together in the glass network. For the glasses considered in this article, the density (ρ) increases systematically by substituting B_2O_3 with Bi_2O_3, as reported in **Table 3**. The obtained data are in excellent agreement with those reported in literature for bismuth borate glasses prepared in Pt crucible [14,18,19].

In order to understand in more detail the role of Bi_2O_3 in the glass network, the molar volume (V_M) and the oxygen packing density (O) were also calculated. From **Table 3**, it is possible to observe that the addition of Bi_2O_3 leads to an increase of V_M and a decrease of O.

By comparing the glasses containing Dy_2O_3 obtained at 1050°C for 1h (1BB-17.5 and 1BB-15) with BB-20 it can be noted that the substitution of Bi_2O_3 by 2.5 and 5 mol% of Dy_2O_3 in the BB-20 produces a weak decrease of density (**Table 4**) from 0 (BB-20) to 2.5 mol% of Dy_2O_3 (1BBD-17.5) followed by a not significant change from 2.5 (1BBD-17.5) to 5mol% (1BBD-15). On the other hand, comparing the BBD17.5 and BBD15 obtained at 1, 3 and 6h it

is possible to note that the density does not have a strong change while the molar volume tends to decrease. The holding time seems to have a very weak effect on the density and the molar volume of BBD-17.5 and BBD-15 as it can be inferred from **Table 4**.

3.3 Differential thermal analysis (DTA)

The DTA spectra (in **Figure 2** the spectrum of BB-20 is illustrated as an example) of all glasses show small and broad crystallization peaks. This suggests a poor tendency to crystallize at a heating rate of 10°C/min used for the DTA analysis, as already reported in other studies on bismuth borate glasses [13]. The glass transition temperature (T_g) within the BB-series tends to diminish from 450°C to 380°C in a non-linear manner, by increasing the Bi_2O_3 content (**Table 3**). In fact, from 20 to 30 mol% of Bi_2O_3 the decrease of T_g is smaller (ca. 20°C) with respect to that observed from 30 to 40 mol% of Bi_2O_3 (ca. 50°C). Concerning the BBD series, the substitution of Bi_2O_3 by Dy_2O_3 in BB-20 composition and the change of the holding time did not produce any variation of T_g (**Table 4**).

3.4 UV/Vis spectroscopy

The study of optical absorption and particularly of absorption edge is a useful method to investigate optically induced electronic transitions and to give information about the band structure and energy gap in both crystalline and non-crystalline materials [20].

The cutoff wavelength (λ_c) and the optical band gap (E_{opt}) were determined from the absorption spectra (**not showed**) in order to analyse possible changes in the glass structure occurring when B_2O_3 is replaced by Bi_2O_3. **Figure 3** shows the Tauc's plot that it is used to determine the direct band gap of the glassy samples. It is observed that E_{opt} decreases with the increase of Bi_2O_3 content from 20 to 30 mol% and at the same time λ_c shifts towards longer wavelengths increasing the content of Bi_2O_3 from 20 to 30 mol%. The glasses doped with Dy_2O_3 did not show particular trend associated to the dysprosium content and to the different holding time. All the transmission spectra show the typical absorption bands of dysprosium

[17,21,22,23]. Particularly, five absorption bands at *ca.* 420, 450, 470 745, 780 nm were observed. In **Figure 4** the spectrum of the BBD-15 glass is illustrated as an example.

3.5 Theoretical optical basicity

Theoretical optical basicity serves, in first approximation, as a measure of the ability of oxygen to donate a negative charge in the glasses. The theoretical optical basicity can be used to classify the covalent/ionic ratios of the glasses since an increase of Λ_{th} indicates a decreasing covalency [24,25]. The theoretical optical basicity (Λ_{th}) was calculated for BB series using eq. (5) previously reported. For the present study Λ_{th} was calculated as illustrated thereafter in eq. (6)

$$\Lambda_{th} = X(BaO)\Lambda(BaO) + X(Bi_2O_3)\Lambda(Bi_2O_3) + X(B_2O_3)\Lambda(B_2O_3) + X(Dy_2O_3)\Lambda(Dy_2O_3) \quad (6)$$

where $X(BaO)$, $X(Bi_2O_3)$, $X(B_2O_3)$ and $X(Dy_2O_3)$ represents the equivalent fractions of the oxides introduced in the glass formulation, while $\Lambda(BaO)$, $\Lambda(Bi_2O_3)$, $\Lambda(B_2O_3)$ and $\Lambda(Dy_2O_3)$ are the optical basicity values of each oxide taken from literature [26]. The Λ_{th} of each BB and BBD glasses are provided in **Tables 3** and **4**, and agree with those reported in literature for bismuth borate glasses [27].

The theoretical optical basicity tends to increase in the BB series by increasing the Bi_2O_3 content, and remains constant by replacing Bi_2O_3 by Dy_2O_3 in the glass formulation. As concern the BBD series no particular trend was found as a function of the holding time used.

3.6 Luminescence properties

In order to obtain the luminescence characteristics of the BBD glasses, excitation and emission spectra were collected. All the excitation spectra of the BBD glasses were recorded by monitoring an emission at about 430 nm and exciting the samples from 350 to 550 nm. The excitation spectra of glasses containing Dy^{3+} (in **Figure 5** the spectrum of 6BBD-15 is reported as an example) showed the excitation peaks of Dy^{3+}, which can be assigned to the

transitions originating from the ground state to the excited ones, as reported in literature [26]. The collected emission spectra showed the presence of luminescent peaks at 480 and 530 nm, respectively (for blue and yellow), well visible only for the sample treated for 6h. In **Figure 6** it is possible to observe that the Dy^{3+} concentration does not affect the position of the different excitation bands for 6BBD-17.5 and 6BBD-15 while it has an influence on the relative intensity of individual peaks, as reported in other works [28].

4. Discussion

The colour change observed in the studied glasses depends on their composition and the melting conditions selected [29]. The first important consideration is related to the dark hug that appears by synthesizing the glasses at 1200°C, independently of the starting composition. The observed darkening effect can be associated to the thermal dissociation of Bi_2O_3 (eq. (5)):

$$2Bi_2O_3 \Leftrightarrow 4Bi^0 + 3O_2 \quad (5)$$

By increasing the melting temperature, the equilibrium shifts toward the lower oxidation state Bi^0 that precipitates as nanoparticles [30]. For the glasses obtained at the melting temperature of 950, 1000 and 1100°C, the origin of coloration might be due to the presence of intermediate species between Bi^{3+} ion and Bi colloids [31,32].

The substitution of B_2O_3 by Bi_2O_3 causes, in the BB series, an increase of both density and molar volume (**Table 3**), that could be mainly attributed to the higher molecular weight of Bi_2O_3 (*i.e.* 465.96 g/mol) with respect B_2O_3 (*i.e.* 69.62 g/mol).

On the other hand, the change of V_M can be also related to the larger values of both the radii and the bond length of Bi_2O_3, compared to those of B_2O_3, which probably cause an increase in bond length or inters atomic spacing. In addition, by increasing the amount of Bi_2O_3 in the glass composition a decrease of T_g (**Table 3**) was detected, the major difference was observed from BB-30 to BB-40. This suggests the probable formation of NBOs in the glass structure, which expand and weaken the borate structure leading consequently to lower T_g values [14].

This hypothesis is also supported by the reduction of the oxygen packing density detected by increasing the Bi_2O_3 concentration, which indicates that the structure at higher bismuth content is loosely packed. As reported in literature, the NBOs formation probably derived from the conversion of BO_4 units into BO_3 ones [27,33,34]. However, it is important to underline that the decrease of T_g can be also described as an increased number of Bi-O linkages which are weaker with respect to B-O ones. The optical absorption spectra of all the glasses indicate the vitreous nature of the samples, as a consequence of the fact that the optical absorption edge is not sharply defined. The optical energy band gap (E_g) and the wavelength (λ_c) were evaluated from their ultraviolet absorption edge. The latter are listed in **Table 3**. By increasing the amount of Bi_2O_3 from 20 (BB-20) to 30 mol% (BB-30), E_g decreases and λ_c shifts at higher wavelength as observed in other works on bismuth borate glasses [20,35,36] while remaining almost constant up to 40 mol%. Both the E_g decrease and λ_c shift suggest structural changes in the glass network, in particular they are an indication of the formation of NBOs in the glass matrix [35,36]. The NBOs contribute to valence band maximum. When a metal-oxygen bond is broken, the bond energy is released and the non-bridging orbitals have higher energies than bonding orbitals. The increase of the NBOs concentration results in shifting of valence band maximum to higher energies, thus reducing the band gap. From the overall results, it can be hypothesized that from BB-20 to BB-30 the bismuth oxide probably acts as a network modifier, thus increasing the NBOs concentration, while from BB-30 to BB-40 other structural changes occur without NBOs formation such as the formation of the Bi-O linkages that are weaker with respect B-O ones. The theoretical optical basicity (Λ_{th}) increases when B_2O_3 is replaced by Bi_2O_3 (**Table 3**), and this can be explained as a higher ability of oxide ions to transfer electrons to the surrounding cations [24], suggesting also an increase of the NBOs [37], especially from BB30 to BB40. The electron donor power of oxygen atoms in the glass is influenced by surrounding cations, especially by

the glass network former. If the bonding of oxygen atom with other cations shows more covalence, the less able that the oxygen donate charge to a solute metal ion in the glass, that is, the smaller the optical basicity of the system.

Thus, from BB-30 to BB40 it is possible to correlate the increase of optical basicity to the formation of more Bi-O linkages in substitution of B-O ones.

As regards to the BBD series, the obtained values of density, molar volume and glass transition temperature (**Table 4**) suggest that probably no strong change occurs in the glass by introducing Dy_2O_3 from 0 (BB-20) to 5 mol% as well as changing the melting time. As previously mentioned, the transmission spectra of all the glasses show the typical absorption bands of Dy^{3+} [21,22,17]. In the glasses considered in this article five absorption bands (optical transitions) at ca. 420, 450, 470 745, 780 nm were observed and their intensities varied according to Dy_2O_3 concentration, as found in other works [21,38]. The change of the melting time in both BBD-17.5 and BBD-15 seems not to produce significant structural rearrangement, however, a major homogeneity in the glasses obtained after 6 hours (6BBD-17.5 and 6BBD-15) at the melting temperature, with respect to those obtained at 1 and 3h, was observed. Thus, for these glasses the luminescence properties were also investigated. The excitation spectra (**Figure 5**) were detected by monitoring the emission at 575 nm and five bands were observed at 363 nm ($^6H_{15/2} \rightarrow {}^4I_{11/2}$), 388 nm ($^4I_{13/2} \rightarrow {}^4F_{7/2}$), 425 nm ($^6H_{15/2} \rightarrow {}^4I_{11/2}$), 450 nm ($^6H_{15/2} \rightarrow {}^4I_{15/2}$), 472 nm ($^6H_{15/2} \rightarrow {}^4F_{9/2}$). The bands assignment was made considering the literature on borate or bismuth borate glasses containing dysprosium oxide [39,40]. Among all the excitation bands the one at 450 nm corresponding to $^6H_{15/2} \rightarrow {}^4I_{15/2}$ is more intense and is was used as an excitation wavelength to record the emission spectra of all the glasses. The luminescence spectra of the samples 6BBD-15 and 6BBD-17.5 (**Figures 6a** and **6b**, respectively) show for both the characteristic band at ca. 480 assigned to the $^4F_{9/2} \rightarrow {}^6H_{15/2}$ (blue) transition of Dy^{3+} ions and another band at *ca.* 530 nm visible only for the sample

containing higher Dy_2O_3 content which can be attributed to the $^4F_{9/2} \rightarrow {}^6H_{13/2}$ (yellow) transition of the same ions [39].

6. Conclusions

Heavy bismuth-borate glasses containing Dy_2O_3 were synthesized and characterized in order to study their potential application as scintillator materials in radiation detectors and, in particular, in high energy physics experiments. The introduction of bismuth in transparent borate glasses leads to the obtainment of a dense material with high transparency making it an interesting system to accommodate scintillating rare earth.

From this study, the following conclusions can be drawn:

1. The glasses change their colour (and thus their optical properties) from pale yellow to dark as a function of composition and processing conditions. The dark hue appears by synthesizing the glasses at 1200°C, independently by the starting composition.
2. The characterization performed on the glass matrix suggests that the substitution of B_2O_3 with Bi_2O_3 leads to the formation of NBOs in the glass structure as well as more Bi-O linkages in substitution of the B-O ones.
3. The introduction of Dy_2O_3 at 2.5 and 5 mol% in substitution of Bi_2O_3 does not produce any significant changes in the glass structure with good density and transparency being preserved.
4. The luminescence spectra of the samples 6BBD-15 and 6BBD-17.5 show for both the characteristic band at ca. 480 assigned to the $^4F_{9/2} \rightarrow {}^6H_{15/2}$ (blue) transition of Dy^{3+} ions and another band at *ca.* 530 nm visible only for the sample containing higher Dy_2O_3 content which can be attributed to the $^4F_{9/2} \rightarrow {}^6H_{13/2}$ (yellow) transition of the same ions.

Acknowledgements

The scientific program “T1015 Collaboration” at Fermilab and the “TWICE project” are greatly acknowledged.

References

[1] G.H. Silva, V. Anjos, M.J.V. Bell, A.P. Carmo, A.S. Pinheiro, N.O. Dantas, J. Lumin. 154 (2014) 294-297.

[2] R.M. Brown, P.S. Flower, J. Fu, J.M. Parker, Nucl. Instr. and Methods A 486 (2002) 303–308.

[3] J. Fu, M. Kobayashi, S. Sugimoto, J.M. Parker, Mater. Res. Bull. 43 (2008) 1502–1508.

[4] J. Fu, M. Kobayashi, J.M. Parker, J. Lumin. 128 (2008) 99–104.

[5] J. M. Park, H.J. Kim, S. Kim, P. Limsuwan, J. Kaewkhao, Procedia Engineering 32 (2012) 855-61.

[6] Y. Zhang, N. Ding, T. Zheng, S. Jiang, B. Han, J. Non-cryst. Solids 441 (2016) 74-78.

[7] A.D. Bross, Nucl. Instr. and Methods A 247 (1986) 319.

[8] R.C. Placious, D. Polansky, H. Berger, C. Bueno, C.L. Vosberg, R.A. Betz, D.J. Rogerson, Mater. Eval. (1991) 1419.

[9] L. ur, J. Janek, M. Sołtys, T. Goryczka, J. Pisarska , W. A. Pisarski J. Non-cryst. Solids 431 (2016) 145–149

[10] H. Lin, E.Y.B. Pun, B.J. Chen, Y.Y. Zhang, J. Appl. Phys. 103 (2008) 056103.

[11] W.A. Pisarski, J. Pisarska, D. Dorosz, J. Dorosz, Mater. Chem. Phys. 148 (2014) 485–489.

[12] O. Maj rus, . Tr gou t, D. Caurant, D. Pytalev, J. Non-cryst. Solids 425 (2015) 91–102.

[13] A. Bishay, C. Maghrabi, Phys. Chem. Glasses 10 (1969) 1.

[14] A. Bajaj, A. Khanna, B. Chen, J. G. Longstaffe, U. W. Zwanziger, J.W. Zwanziger, Y. me z, F. onz lez, J. Non-cryst. Solids 355 (2009) 45–53

[15] J. Massera, M. Gaussiran, P. Glucowsky, M. Lastusaari, L. Petit, J. Holsa, L. Hupa, Opt. Mater. 52 (2016) 56-61.

[16] J.A.Duffy, M.D.Ingram, J.Non-cryst.Solids 249 (1999) 160.

[17] R. S. E. S. Dawaud, S.Hashim, Y.S.M. Alajerami, M.H.A. Mhareb, N. Tamchek, J. Mol. Struct. 1075 (2014) 113–117.

[18] M. Farouk, A. Samir, F. Metawe, M. Elokr , J. of Non-Cryst. Solids 371–372 (2013) 14–21.

[19] Y.B. Saddeek, E.R. Shaaban, E. Moustafa, H.M. Moustafa, Physica B 403 (2008) 2399–2407.

[20] M. Subhadra and P. Kistaiah, J. Phys. Chem. A 2011, 115, 1009–1017

[21] T. Ying Lim, H. Wagiran, R. Hussin, S. Hashim , M.A. Saeed, Physica B 451 (2014) 63–67.

[22] P. Babu, C.K. Jayasankar, Opt. Mater. 15 (2000) 65.

[23] S. Insitipong, J, Kaewkhao, T. Ratana,P. Limsuwan, Procedia Ingineering 8 (2011) 195-99

[24] S. Insiripong, P. Chimalawong, J. Kaewkhao, P. Limsuwan, American Journal of Applied Sciences 8 (2011) 574-578.

[25] Li-Hua Zheng, Xin-Yuan Sun, Ri-Hua Mao, Hao-Hong Chen, Zhi-Jun Zhang, Jing-Tai Zhao, J. Non cryst. Solids 403 (2014) 1-4

[26] V. Dimitrov and S. Sakka, J Appl. Phys. 79 (1996) 1736-40.

[27] S.R. Rejisha, N. Santha, J. Non-cryst. Solids 357 (2011) 3813–3821

[28] L. Mishra , A.Sharma, Amit K. Vishwakarma, K. Jha, M. Jayasimhadri, B.V. Ratnam, K. Jang, A.S. Rao, R.K. Sinha, J. Lumin. 169 (2016) 121–127

[29] O. Sanz, E. H. Poniatowsky, J. Gonzalo, J. M. F. Navarro, J. Non-cryst. Solids 352, (2006) 761.

[30] S. Khonthon, S. Morimoto, Y. Arai, Y.Ohishi, Optical Materials 31 (2009) 1262–1268.

[31] A. Paul, Chemistry of Glass, Chapman and Hall, London, 1990. pp. 218–245.

[32] S. Khonthon, S. Morimoto, Y. Arai, Y. Ohishi, Opt. Mater. 31 (2009) 1262–1268.

[33] D. Saritha, Y. Markandeya, M. Salagram, M. Vithal, A. K. Singh, and G. Bhikshamaiah, J. Non-cryst. Solids, vol. 354, no. 52–54, pp. 5573–5579, 2008.

[34] C. Stehle, C. Vira, D. Hogan, S. Feller, M. Affatigato Phys. Chem. Glasses 39 (1998) 83-86

[35] S. Sindhu, S. Sanghi, A. Agarwal, V. P. Seth, N .Kishore, Mater. Chem. Phys. 90 (2005) 83-89

[36] S. Rani, S. Sanghi, A. Agarwal, N. Ahlawat, J. Alloys Compd. 477 (2009) 504.

[37] Shamsi Sadat Alavi Qazvini, Zohreh Hamnabard, Zahra Khalkhali, Saeid Baghshahi, Amir Maghsoudipour, Ceram. Int. 38 (2012) 1663–1670.

[38] Manpreet kaur, Anupinder Singh, Vanita Thekur, Lakjwant Singh, Opt. Mater. 53 (2016) 181-189

[39] M. A. Marzouk, J. of Molecular structure 1019 (2012) 80-89.

[40] M.V. Sasi kumar, D. Rajesh, A. Balakrishna, Y.C. Ratnakaram, J. Mol. Struct. (2013) 100–105.

Figure captions

Figure 1. X-Ray diffraction pattern of the BB-20 glass

Figure 2. DTA spectrum of the BB-20 glass

Figure 3. Extrapolation of optical band gap energy (E_{opt}) for all the BB glasses

Figure 4. UV/Vis spectrum of BBD-15 glass

Figure 5. Excitation spectrum of 6BBD-15 glass

Figure 6. Emission spectra (λ_{ex} = 400nm) of **a)** 6BBD-15 and **b)** 6BBD17.5 glasses

Table

Table 1. Ternary glass compositions (expressed in mol%), sample ID, melting temperature (T_M) and appearance

Composition	Sample ID	T_M (°C)	Appearance
$20BaO\text{-}20Bi_2O_3\text{-}60B_2O_3$	BB-20	950	Pale yellow
$20BaO\text{-}20Bi_2O_3\text{-}60B_2O_3$		1050	Pale yellow
$20BaO\text{-}20Bi_2O_3\text{-}60B_2O_3$		1100	Light yellow
$20BaO\text{-}20Bi_2O_3\text{-}60B_2O_3$		1200	Dark
$20BaO\text{-}30Bi_2O_3\text{-}50B_2O_3$	BB-30	950	Light Yellow
$20BaO\text{-}30Bi_2O_3\text{-}50B_2O_3$		1050	Amber
$20BaO\text{-}30Bi_2O_3\text{-}50B_2O_3$		1100	Amber
$20BaO\text{-}30Bi_2O_3\text{-}50B_2O_3$		1200	Dark
$20BaO\text{-}40Bi_2O_3\text{-}40B_2O_3$	BB-40	950	Amber
$20BaO\text{-}40Bi_2O_3\text{-}40B_2O_3$		1050	Amber
$20BaO\text{-}40Bi_2O_3\text{-}40B_2O_3$		1100	Amber
$20BaO\text{-}40Bi_2O_3\text{-}40B_2O_3$		1200	Dark

Table 2. Compositions of glasses containing Dy_2O_3 (expressed in mol%), holding times tested at the melting temperature of 1050°C and sample ID

Composition	Holding time (h)	Sample ID
$20BaO\text{-}17.5Bi_2O_3\text{-}60B_2O_3\text{-}2.5Dy_2O_3$	1	1BBD-17.5
$20BaO\text{-}17.5Bi_2O_3\text{-}60B_2O_3\text{-}2.5Dy_2O_3$	3	3BBD-17.5
$20BaO\text{-}17.5Bi_2O_3\text{-}60B_2O_3\text{-}2.5Dy_2O_3$	6	6BBD-17.5
$20BaO\text{-}15Bi_2O_3\text{-}60B_2O_3\text{-}5Dy_2O_3$	1	1BBD-15
$20BaO\text{-}15Bi_2O_3\text{-}60B_2O_3\text{-}5Dy_2O_3$	3	3BBD-15
$20BaO\text{-}15Bi_2O_3\text{-}60B_2O_3\text{-}5Dy_2O_3$	6	6BBD-15

Table 3. Density (ρ), molar volume (V_M), glass transition temperature (T_g), oxygen packing density (O), optical energy band gap (E_{opt}), cut off (λ_{cutoff}) and theoretical optical basicity (Λ_{th}) values of the BB series obtained at 1050°C

Sample ID	BB-20	BB-30	BB-40
ρ (g/cm^3) (± 0.01)	5.21	6.05	6.67
V_M (cm^3mol^{-1}) (± 0.01)	31.77	33.91	36.72
T_g (°C) (± 5)	450	430	380
O (g-atm /l)	81.8	76.7	70.8
E_{opt} (eV)	2.7	2.3	2.3
λ_c (nm)	380	410	410
Λ_{th} (± 0.02)	0.736	0.813	0.974

Table 4. Density (ρ), molar volume (V_M) and glass transition temperature (T_g) values of the BBD series melted at 1050°C at different holding times (1, 3, 6 h)

Sample ID	**1BBD-17.5**	**3BBD-17.5**	**6BBD-17.5**	**1BBD-15**	**3BBD-15**	**6BBD-15**
ρ (g/cm^3) (± 0.01)	5.04	4.85	4.88	5.05	5.10	5.06
V_M (cm^3mol^{-1}) (± 0.01)	32.54	33.65	33.50	31.88	31.56	31.81
O (g-atm/l)	80.2	77.2	77.7	81.6	82.4	81.7
T_g (°C) (± 5)	440	450	440	420	430	450
Λ_{th} (± 0.02)*	0.73			0.72		

**the* Λ_{th} values are reported one time since they are independent from the different holding times

Figure 1

Click here to download high resolution image

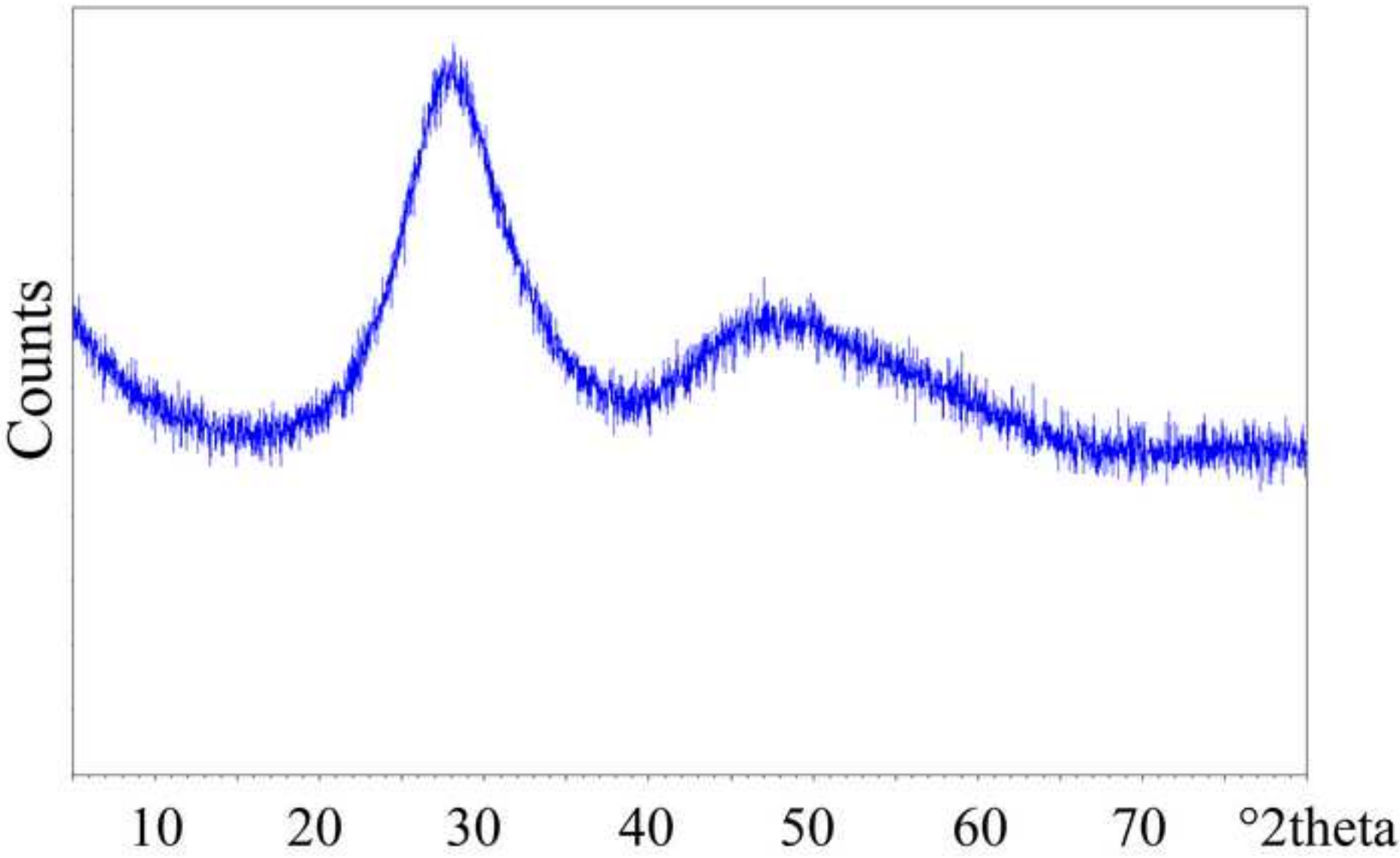

Figure 2
Click here to download high resolution image

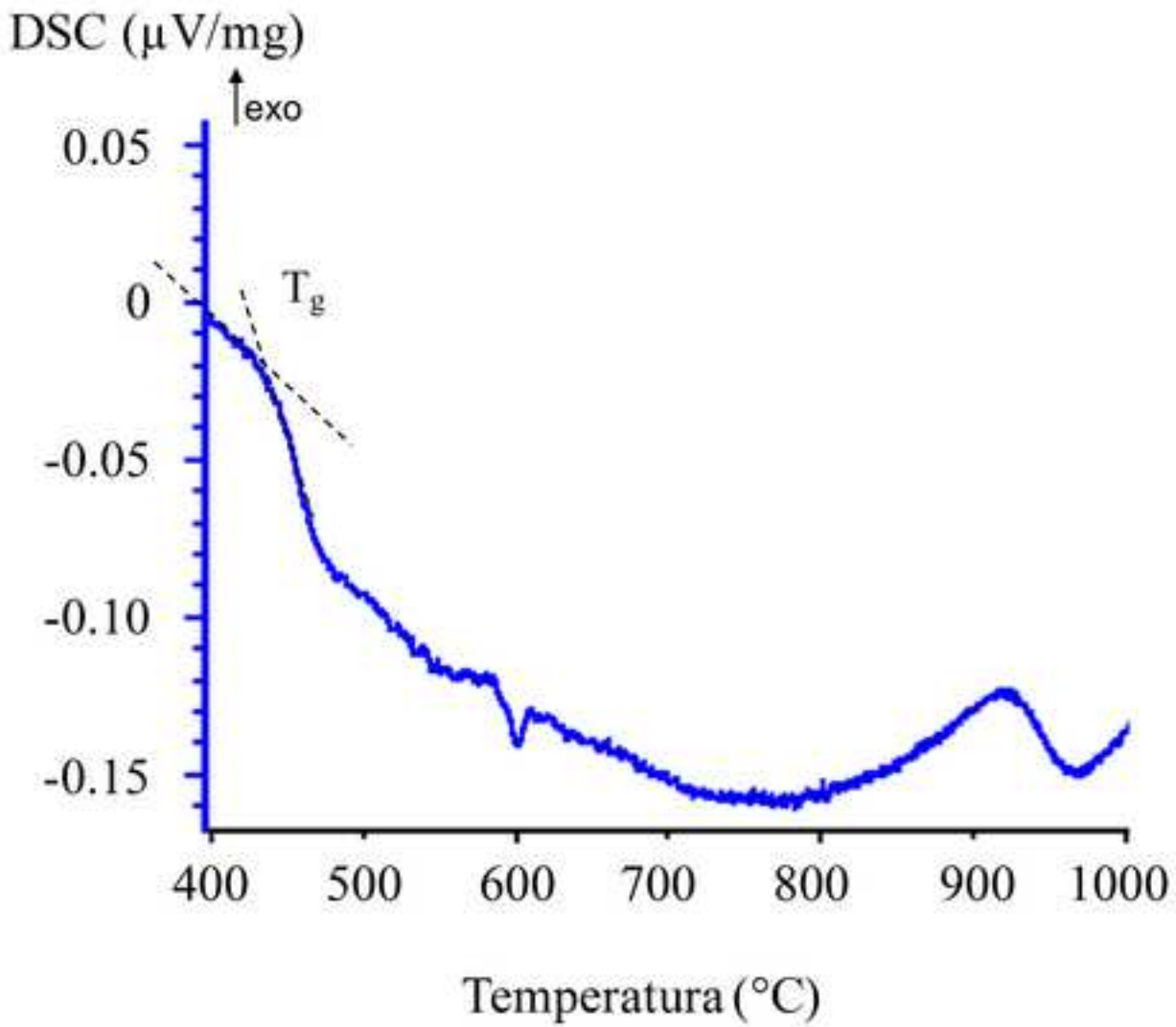

Figure 3
Click here to download high resolution image

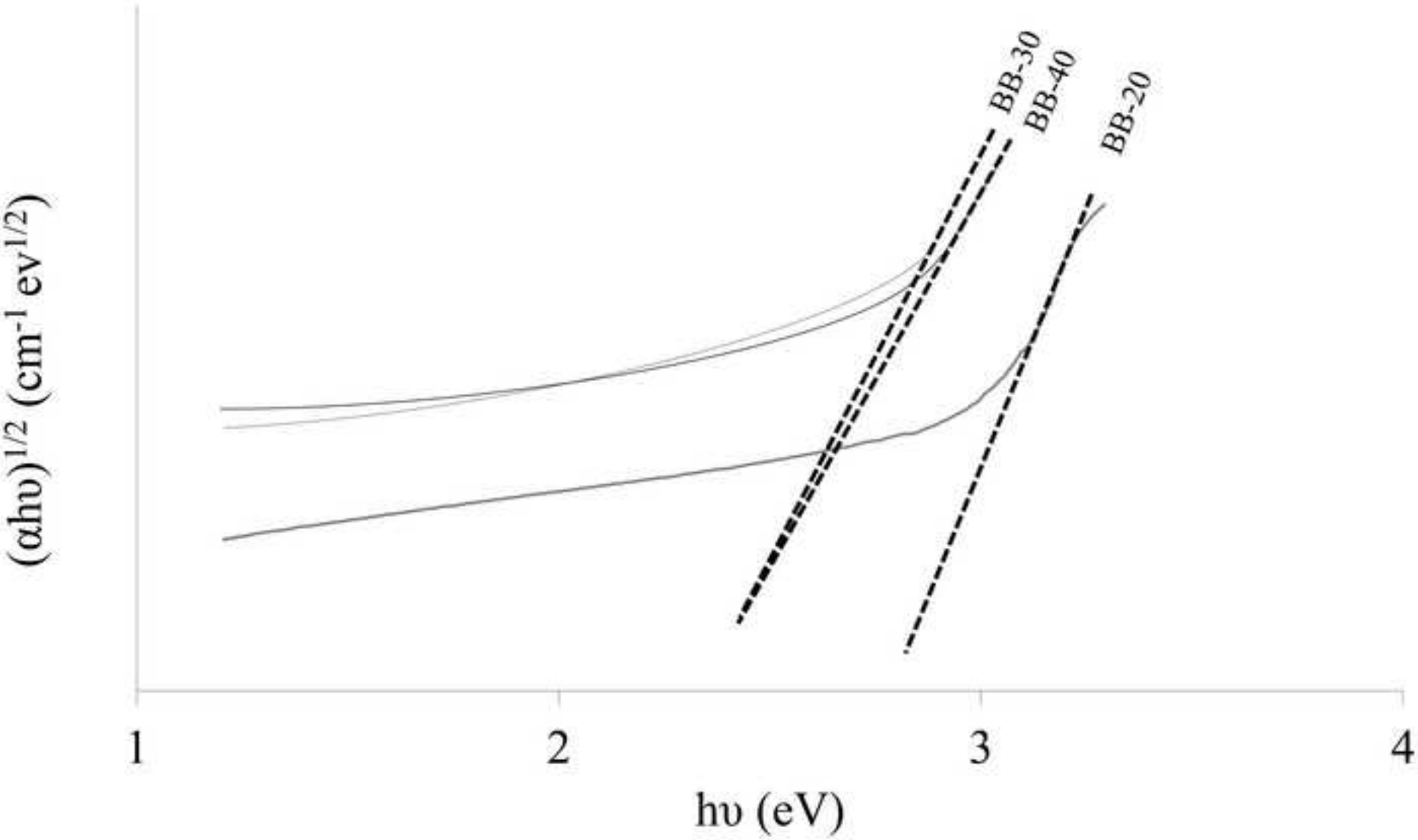

Figure 4

Click here to download high resolution image

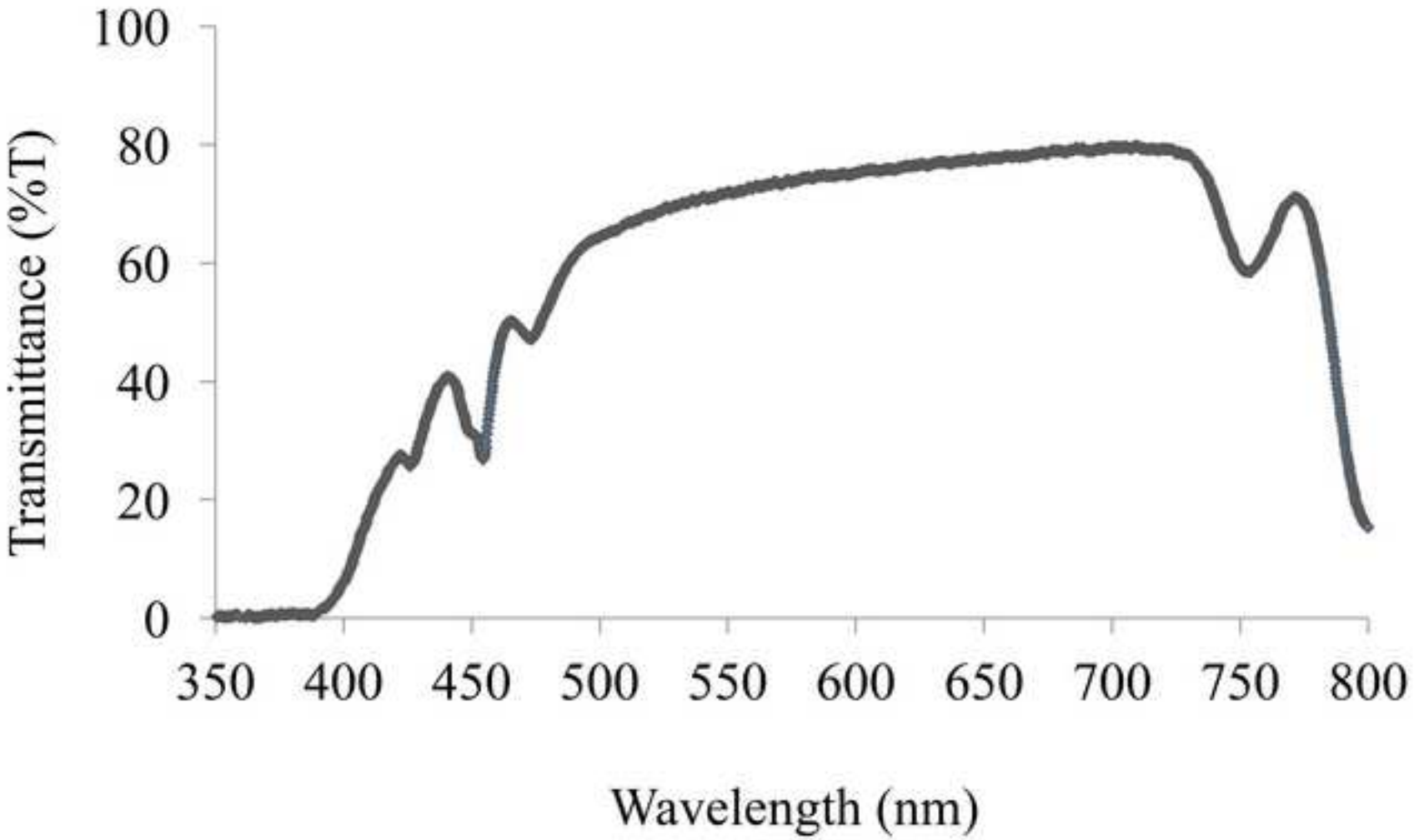

Figure 5
Click here to download high resolution image

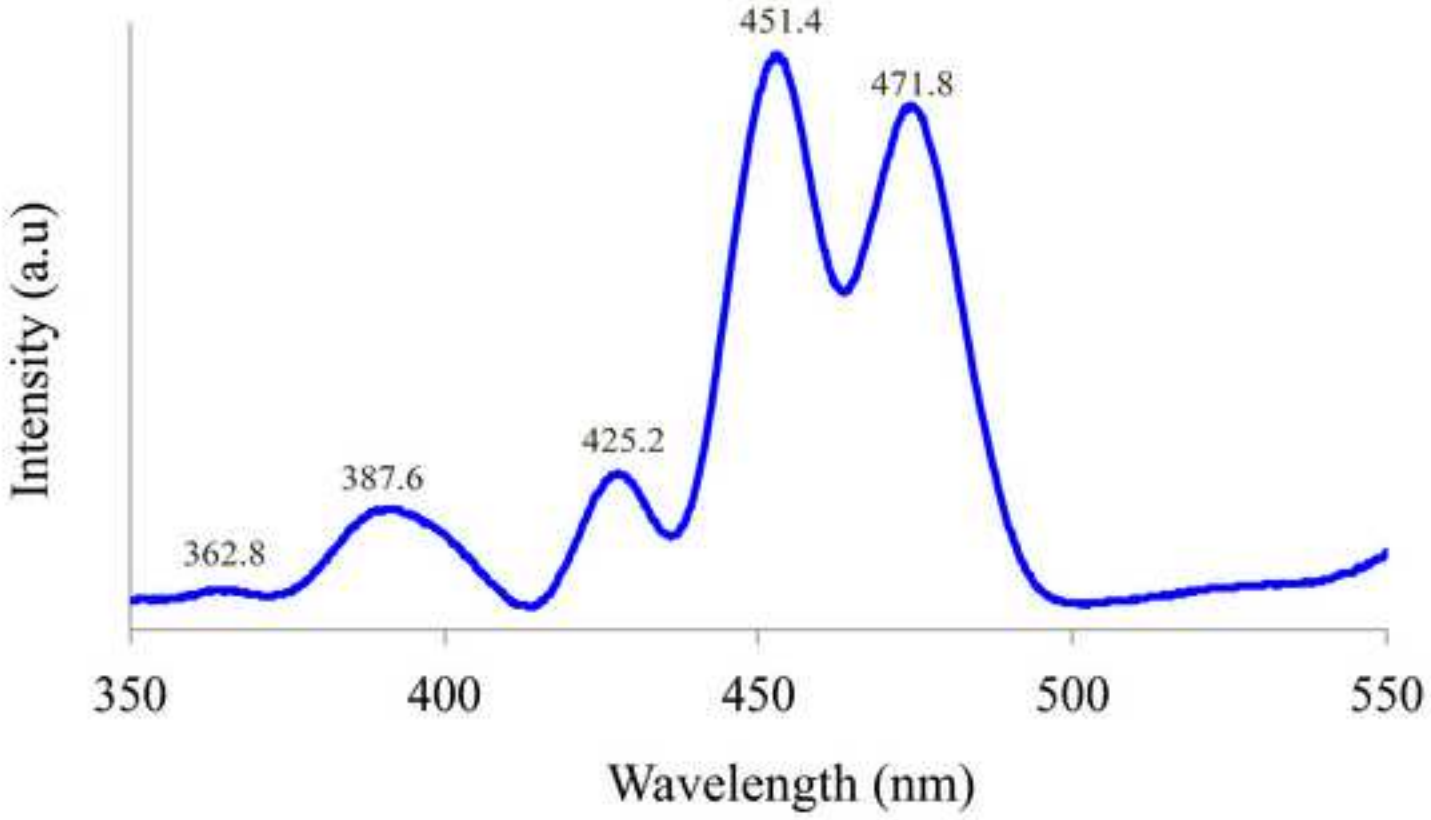

Figure 6a

Click here to download high resolution image

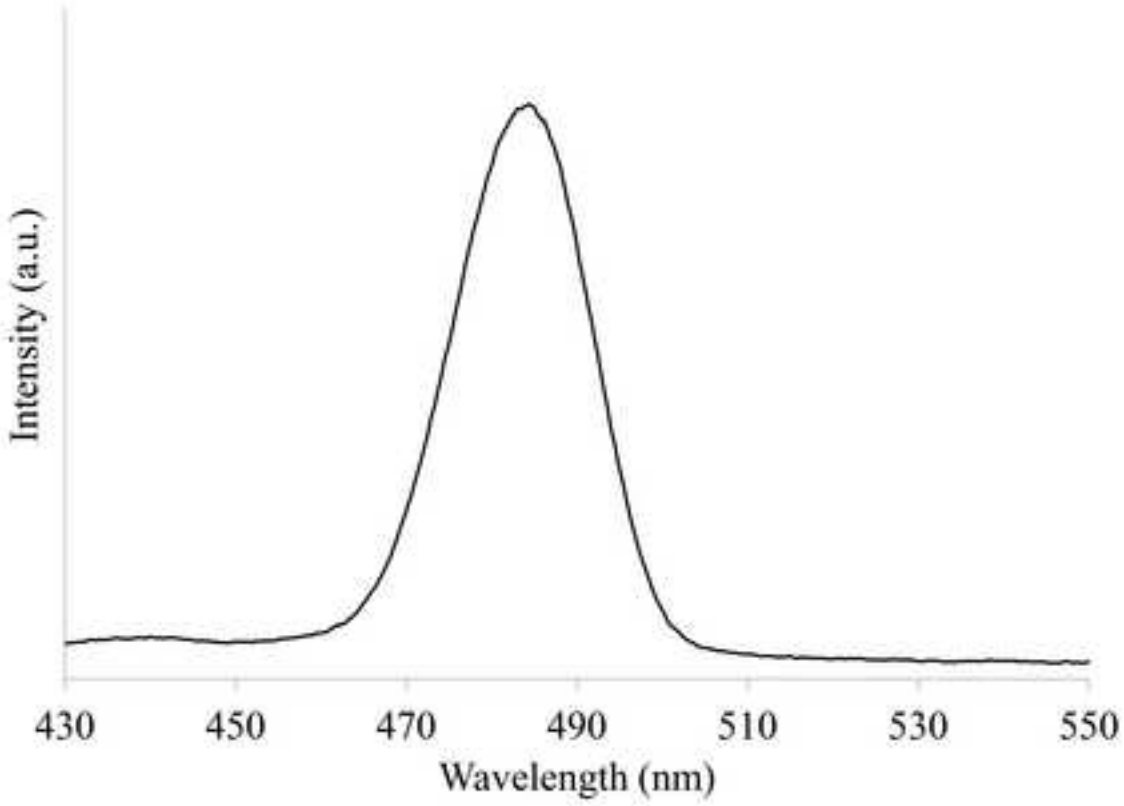

Figure 6b
Click here to download high resolution image